Environment International 139 (2020) 105712

Contents lists available at ScienceDirect

Environment International

journal homepage: www.elsevier.com/locate/envint

Changing nature of Saharan dust deposition in the Carpathian Basin (Central Europe): 40 years of identified North African dust events (1979–2018)

György Varga

Research Centre for Astronomy and Earth Sciences, Budapest H-1112, Hungary

ARTICLE INFO

Keywords:
Saharan dust events
Carpathian Basin
Dust deposition
Grain size

ABSTRACT

Several billion tonnes of mineral dust is emitted, and transported through winds every year from arid-semiarid areas. North African dust hot spots located in the Sahara are responsible for 50–70% of the global mineral dust budget. Dust-loaded air-masses originated from these sources can be transported over long distances and can also affect remote areas, such as North and South Americas, Europe, and the Middle East.

In this study, we analysed 218 identified Saharan dust events (SDEs) in the Carpathian Basin (Central Europe) during 1979 to 2018. Systematic identification of SDEs and analyses of dust emission, dust source area activity, dust transporting wind systems, and transport routes revealed that different synoptic meteorological patterns are responsible for SDEs, and these are occurring mostly in spring and summer. The characteristic synoptic meteorological background of episodes was also identified, and three major types of atmospheric pressure-system patterns were distinguished.

In recent years, several intense wintertime dust deposition events have been recorded in Central Europe. All of the identified unusual episodes were characterised by severe washout of mineral dust material and were related to very similar synoptic meteorological situations. Enhanced southward propagation of a high-latitude upper-level atmospheric trough to north-western Africa and orographic blocking of Atlas Mountains played an essential role in the formation of severe dust storms, whereas the long-range transport was associated with the northward branch of the meandering jet. The occurrence and southerly penetration of high-latitude upper-level atmospheric trough to low-latitudes and the increased meridionality of the dominant flow patterns may be associated with enhanced warming of the Arctic, leading to more meandering jet streams.

Particles size of sampled dust material of some intense deposition episodes were very coarse with a considerable volumetric proportion of $>$ 20 μm particles.

1. Introduction

Atmospheric mineral dust is a vital component of the Earth's climatic system. Similar to other aerosol constituents, dust particles are regarded as ones of the less known drivers of recent climatic changes. According to the reports of the Intergovernmental Panel on Climate Change (IPCC), because of their observational uncertainties, aerosols hamper attribution of changes of the climatic system (Boucher et al., 2013; Regayre et al., 2018; Penner, 2019). Dust particles with diverse sizes, shapes, mineralogies, degrees of aggregation, and optical properties play an intricate role in the energy balance of the Earth. Dust particles can absorb, scatter, and reflect the incoming shortwave and outgoing longwave radiation, perturbing the radiation budget of the Earth-atmosphere system (Sokolik and Toon, 1996; Pérez et al., 2006a; Huang et al., 2014; Nabat et al., 2015; Ginoux, 2017; Gkikas et al., 2018, 2019). Dust particles serve as cloud condensation nuclei and ice nuclei, affecting the formation, structure, and properties of clouds and precipitation, indirectly altering the net radiation (Twomey, 1974; Albrecht, 1989; Yu et al., 2006). Dust particles deposited on snow and ice-covered surfaces can darken the surface, affect the surface energy balance, and accelerate snow/ice melting (Drake, 1981; Reynolds et al., 2014). Dust deposition also brings essential nutrients, which affect the terrestrial and aquatic biogeochemical cycles and hence the climate (Meskhidze et al., 2005; Fan et al., 2006; Schulz et al., 2012).

Several billion tonnes of mineral dust is emitted every year from arid-semiarid areas and are transported up to several thousands of kilometres by winds. North African dust hot spots located in the Sahara and Sahel contribute to 50–70% of the global mineral dust budget (Ginoux et al., 2001). Dust-loaded air-masses originated from these sources also affect remote areas; vast amounts of mineral particles are transported to North and South Americas across the Atlantic Ocean, toward the Middle East, and in the direction of Europe. The PM2.5 and

E-mail address: varga.gyorgy@csfk.mta.hu.

https://doi.org/10.1016/j.envint.2020.105712
Received 31 December 2019; Received in revised form 19 March 2020; Accepted 31 March 2020
Available online 10 April 2020

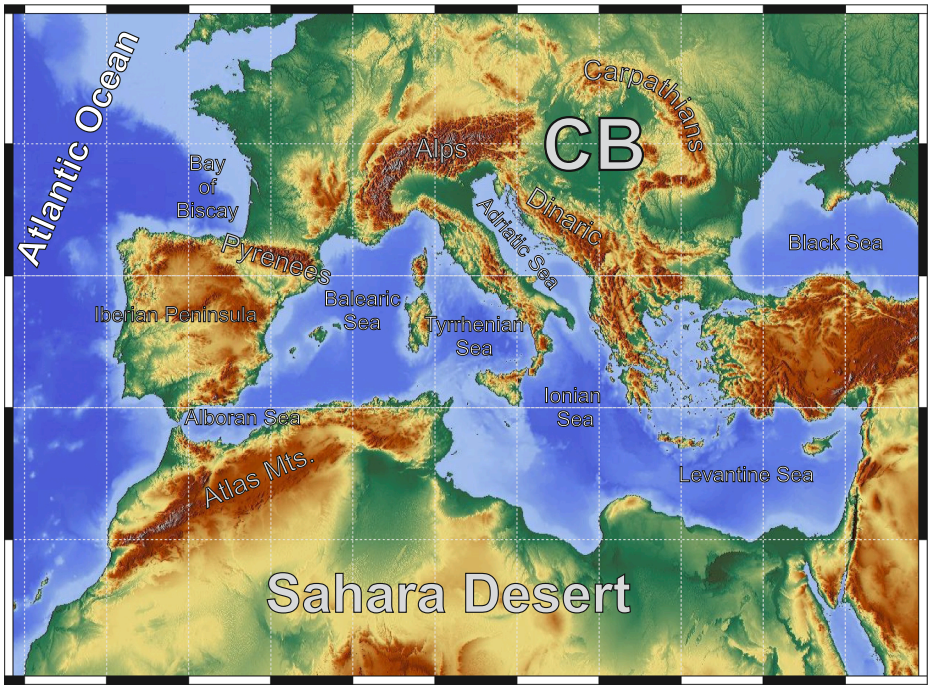

Fig. 1. Location map of the study area (CB: Carpathian Basin).

PM10 levels of Southern European countries (e.g., Spain, Italy, and Greece) often exceed the European Union standards during intense Saharan dust events (SDEs) (Rodríguez et al., 2001; Gerasopoulos et al., 2006; Matassoni et al., 2011; Pey et al., 2013; Pandolfi et al., 2014; Querol et al., 2009). According to Querol et al. (2019), increases in particulate matter concentration were also associated with mixing layer height reductions during SDEs. In addition to other health effects (e.g., respiratory problems and skin and eye irritation), even mortality and morbidity increases were reported during SDEs by several authors (e.g., Perez et al., 2008; Tobías et al., 2011). Other environmental effects of atmospheric and deposited Saharan dust are also widely investigated in the Mediterranean area; cloud formation (Di Biagio et al., 2009; Klein et al., 2010; Bangert et al., 2012; Smoydzin et al., 2012), acid rain (Rodá et al., 1993; Rogora et al., 2004), lake salinity (Psenner, 1999), and even soil-forming processes are considerably modified by the mineral particles transported from North African deserts (Yaalon and Ganor, 1973; MacLeod, 1980; Atalay, 1997; Yaalon, 1997; Durn et al., 1999; Muhs et al., 2010).

Measurement campaigns of Saharan dust in the Mediterranean have been provided both by passive satellite-borne sensors (Moulin et al., 1998; Husar et al., 1997; Herman et al., 1997; Dulac et al., 1992), by active spaceborne retrievals (Amiridis et al., 2013; Gkikas et al., 2016), and by lidar measurements (Mona et al., 2006; Papayannis et al., 2008). Daily satellite aerosol measurements have shown that Saharan dust is an important constituent of the Mediterranean atmosphere, where North African dust loads were identified in 23.5% of long-term daily observations in the Western basin (Alboran and Balearic Seas), in 29.5% in the Central Mediterranean (Tyrrhenian and Ionian Seas and Sea of Sicily), and 33.75% in the Eastern Mediterranean by Varga et al. (2014a). Moreover, British Isles (Burt, 1991; Vieno et al., 2016), Germany (Klein et al., 2010), and Scandinavian areas (Franzén et al., 1994, Barkan and Alpert, 2010) are also affected by the mineral dust intrusions from North Africa. Furthermore, European countries in Central Europe are also affected by Saharan dust (Borbély-Kiss et al., 2004, Koltay et al., 2006, Szoboszlai et al., 2009; Varga et al., 2013, 2014b, 2016). Mineral dust deposition in the high mountainous areas of the Alps and Carpathians could lead to accelerated snow melting as a result of snow albedo modification of dust material and as a consequence of snow algae formation (Di Mauro et al., 2015, 2019; Greilinger et al., 2018). The role of past Saharan dust deposition in soil formation has already been studied in the Central European loess-paleosol sequences by Varga et al. (2016). Because of the missing long-term dust deposition measurements in the region, the pedogenic importance of the Saharan dust flux cannot be quantified. In general, Central Europe lies in the D1b zone (meaning dust 'admixture zone') of the 'Saharan dust-fall map' proposed by Stuut et al. (2009), implying that recent Saharan dust material can be incorporated into the soil system and may increase its fine silt content.

Previous long-term investigations revealed a clear seasonal pattern of SDEs affecting Central Europe based on 130 identified episodes (Varga et al., 2013). This analysis of daily aerosol index data from 1979 to 2011 indicated the spring- and summertime maxima of mineral dust episodes in the broader area of the Carpathian Basin (Varga et al., 2013). Systematic analyses of dust emission, dust source area activity, dust transporting wind systems, and transport routes revealed that different synoptic meteorological patterns are responsible for SDEs. The characteristic synoptic meteorological background of SDEs was also identified, and three major types of atmospheric pressure-system patterns were distinguished.

In recent years, several intense wintertime dust deposition events have been recorded in the investigation area (Varga et al., 2014b). In this study, our objectives are to (1) expand and complete the previously established simple SDE time-series (by Varga et al., 2013) for the 40 years from 1979 to 2018; (2) explain the major causes and drivers of the recent extreme and unusual dust deposition episodes; (3) discuss the possible role of recent climatic changes in the changing intensity of wintertime dust deposition in Central Europe; (4) provide information regarding dust deposition; and (5) discuss unresolved problems and possible connections of grain size and dust deposition.

2. Methods

2.1. Study area

The Carpathian Basin (CB: 45°–48.5° N, 16°–23° E) is located in Central Europe and its subsiding depression is framed by the Alps, the

Carpathians, and the Dinaric mountain ranges (Fig. 1). The geomorphological character of the basin is dominated by plains and gently hilly regions with mountain ranges generally below 1000 m a.s.l.; low relief and poor vertical dissection describe the topography. The 1,500-km long ranges of Carpathians (adjoining to the Alps in the west and to the Dinaric in the south) represent the high mountainous frame for the basin. The general climatology of the study area is described by Atlantic, Mediterranean, and continental effects. According to ensembles of regional climate models (considering the intermediate A1B emission scenario), hot and dry summers, moist winters, and increased water transport from lower latitudes are expected in the Carpathian Basin; the dominance of the Mediterranean climate regime influence will increase (Kis et al., 2017).

2.2. Satellite measurements

For appropriate monitoring of recent Saharan dust events, aerosol products of several satellite campaigns were used. The long-term daily aerosol measurements of NASA's Total Ozone Mapping Spectrometer (TOMS Nimbus-7 TOMSN7L3 v008; TOMS Earth-Probe TOMSEPL3) and Ozone Monitoring Instrument (OMI – Daily Level 3 Gridded Products; OMTO3d – source: NASA Goddard Earth Sciences Data Information Services Center (GES DISC) via Giovanni online (Web) environment for the display and analysis of geophysical parameters https://giovanni.gsfc.nasa.gov/) were applied. The TOMS Aerosol Index (AI) and OMI's TOMS-like AI measure the relative amount of aerosols based on the differences in the measured backscattered ultraviolet radiation of the atmosphere (containing aerosols) and a calculated pure molecular atmosphere. Its positive values indicate absorbing aerosols (dust, smoke from biomass burning, and volcanic aerosols). As a result of the geographical location of the investigation area (Carpathian Basin is situated far from active volcanoes, and in common agricultural practices in the European countries, biomass burning is not applied), positive values mostly indicate mineral dust. TOMS and OMI TOMS-like AI measurement series have been used by several previous studies to identify dust events and source areas (e.g. Prospero et al., 2002; Washington et al., 2003; Gao and Washington, 2009; Gkikas et al., 2009, 2013, 2016; Varga, 2012; Varga et al., 2013, 2014a).

The daily AI values of the investigation area (45°–48.5°N, 16°–23°E) were standardised following the work of Barkan (2005); $AI_{st} = (AI - AI_{mean})/\sigma_{AI}$, where AI_{st} is the daily standardised AI value, AI_{mean} is the yearly regional mean AI, and σ_{AI} is the standard deviation. A negative value of AI_{st} indicates below-average values, whereas positive values represent possible dusty episodes. The periods of 2001–2004 and 2010–2011 could not be analysed in the same way because of calibration problems; for these intervals, the initial selection of possible SDEs was performed directly from daily graphical AI maps. The fractional data of AI of 1993 and 1996 (caused by satellite failure) were used in our work, but the years with missing data (1994 and 1995) had to be excluded from the long-term analyses.

As the satellite-based dust detection over land surfaces, especially in mid- and high-latitude regions, is rather complicated due to local aerosol emissions and cloud cover, additional confirmation is needed to identify SDEs. Possible SDE-days were initially selected based on the AI_{st} values, but SDE-days were only accepted after being confirmed by backward-trajectory calculations, where the Saharan surface origin had to be established both from the path of the trajectories and from the vertical profiles of air-mass transport. Multiple endpoints from different heights (1500, 3000, and 4500 m a.s.l.) were used during the 72–120 h backward-trajectory analyses, performed by NOAA HYSPLIT (HYbrid Single-Particle Lagrangian Integrated Trajectory) model to determine the main dust transportation pathways (Stein et al., 2015; Rolph et al., 2017). The meteorological input for the trajectory model was also obtained from the NCEP/NCAR (National Centers for Environmental Protection/National Center for Atmospheric Research) Reanalysis Project dataset (Kalnay et al., 1996).

Atmospheric presence of mineral dust was also verified by true colour satellite images of NOAA Advanced Very High Resolution Radiometer (AVHRR), ESA Meteosat Spinning Enhanced Visible and Infrared Imager (SEVIRI), or Terra/Aqua Moderate Resolution Imaging Spectroradiometer and Aerosol Optical Depth data (NASA MODIS Aqua/Terra), from 2000 dust models (BSC-DREAM8, NMMB/BSC-Dust-model, and SKIRON; results of numerical simulations were not applied by Varga et al., 2013), and surface observations at the proposed source areas (visibility-reducing surface weather reports of Naval Research Laboratory: https://www.nrlmry.navy.mil/aerosol/#aerosolobservations) were also applied in the verification procedure. Verification of episodes from the '80 s and '90 s was based on much fewer available data sources, but AI_{st} and back-trajectories were used as the basis of identification.

Direct values of AI and AI_{st} are also on aerosol optical thickness, single scattering albedo, aerosol layer height, and underlying surface albedo. Thus, these indices can be used only as qualitative descriptors of mineral dust and not as direct, quantitative ones. AI_{st} was used solely for identification of dust and not for assessment of concentration or amount. In this sense, difficult compliance of numerical values of the different satellites and sensors (discussed in detail by Gassó and Torres, 2019) did not cause problems. Consecutive SDE-days (with the verified atmospheric presence of mineral dust) were registered as individual episodes.

2.3. Numerical simulations

In contrast to the dust load, there is much less information regarding dust deposition. Although dust has long been observed in the Mediterranean and Europe, it remains uncertain about how much dust is transported to the region and how much and where the dust is deposited. There are very few direct measurements of Saharan dust deposition in Europe. Therefore, estimates of dust flux were performed via model calculations using the data of BSC-DREAM8b (Barcelona Supercomputing Center's Dust REgional Atmospheric Model) v1.0 and v2.0 and Non-hydrostatic Multiscale Model NMMB/BSC-dust models and a mineral dust model database. Simulation results of the BSC-DREAM8b v1.0 are available from 1 January 2000 to 31 December 2012, whereas the results of the updated v2.0 calculations are ready for the period between 1 January 2006 and 31 December 2014. The BSC-DREAM8b models predict the atmospheric residence of the eroded fine-grained aeolian material by solving Euler-type partial differential non-linear equations. The meteorological fields are initialised every 24 h, while the boundary conditions are updated every 6 h (Pérez et al., 2006a, 2006b; Basart et al., 2012). The available numerical time series is short; however, it has to be considered because modelled daily values of BSC-dust models have already been proven to represent the atmospheric dust load well (Haustein et al., 2009, 2012; Pérez et al., 2011; Di Tomaso et al., 2017) and the simulated values are the only useable quantitative data sources of daily dust deposition in the area (Varga et al., 2016).

NASA's Modern-Era Retrospective analysis for Research and Applications, Version 2 (MERRA-2) provides modelled monthly data from 1980 (Gelaro et al., 2017). Summarised dry and wet deposition data of the five available dust size-bins of the model were obtained from NASA Goddard Earth Sciences Data Information Services Center (GES DISC) via Giovanni application for visualisation and access Earth science remote sensing data (https://giovanni.gsfc.nasa.gov/giovanni/).

2.4. Synoptic background

To define the synoptic meteorological patterns associated with dust intrusion episodes in the investigation area, mean geopotential height (700 hPa), wind vector, meridional, and zonal flow maps as well as a 250-hPa jet stream wind flow map were compiled for the dusty days using the Daily Mean Composite application of NOAA Earth System Research Laboratory (http://www.esrl.noaa.gov/psd/). According to

previous studies, the 700 hPa level represents the typical dust transport altitude (Alpert et al., 2004; Barkan, 2005; Varga et al., 2013, 2014a).

Days with meridional wind components exceeding 10 and 15 m/s at 700 hPa were investigated for every decade and season to uncover possible strengthening of the atmospheric flow meridionality in Central Europe and in the Central Mediterranean. Thresholds were defined based on the compiled meridional flow maps of individual SDEs, where 10 and 15 m/s isotachs indicated the strongest flow and main pathways of dust transport. Surface air temperature anomalies (based on 1981–2010 climatology) were also calculated using the gridded NCEP/NCAR (National Centers for Environmental Protection/National Center for Atmospheric Research) Reanalysis Project dataset (Kalnay et al., 1996) for Central Europe.

2.5. Grain size of deposited dust material

Grain sizes of the collected mineral dust samples of six intense dust episodes were measured by applying a Malvern Morphologi G3-ID automated static image analyser and a laser diffraction method of Malvern Mastersizer 3000 with a Hydro-Lv unit. For appropriate characterisation, ~0.5 g of dust material was required for laser diffraction. At the same time, the image analyser directly measured the size and shape parameters of individual particles. It also provided robust statistical data based on a few hundred thousand mineral grains (less than 0.1 g); a detailed description of the granulometric procedure can be found in Varga et al. (2018). In most cases, it was not possible to collect 0.5 g of Saharan dust material, even after very intense washout episodes.

3. Results

3.1. General patterns of SDEs in the Carpathian Basin

As a result of the systematic analysis of satellite measurements completed with the above-detailed verification process, 218 SDEs were identified between 1979 and 2018. The previous study of Varga et al. (2013) was completed with 88 new dust episodes. SDEs of these 40 years (years 1994 and 1995 missing due to satellite failures, while 1993 and 1996 are only represented as fractional years) showed diverse interannual distribution with a substantial increase in the last decade. The seasonality of the episodes is dominated by spring and summer dust events coinciding with the dust activity of Saharan source areas. According to Israelevich et al. (2002), there is an almost permanent reservoir of atmospheric dust during summer and spring over the main Saharan source regions. Dust transport from North Africa is primarily governed by the synoptic meteorological situations of the broader region determining the upper-level wind flow patterns. Similar seasonal distribution of the dust storms was also reported for the Western and Central Mediterranean by Gkikas et al. (2009, 2013, 2016), Querol et al. (2009), Pey et al. (2013), and Varga et al. (2014a).

SDEs were classified into three main synoptic meteorological types based on the daily 700 hPa geopotential height, wind maps, and dust transport pathways of SDEs. The different types were defined by specific deterministic atmospheric patterns: Type-1 SDEs were connected to deep atmospheric troughs over Western Europe and north-western Africa; dust transport of Type-2 episodes was caused by Central Mediterranean cyclones; Type-3 events were defined based on the rare dust transport, when dust-loaded air-masses approached the Carpathian Basin from the north-western directions (Figs. 2-3.).

Type-1 episodes have been determined by the south-western flow created by a deep trough (emanated from south-western Europe to the Atlantic coast of N-Africa) and the subdivided subtropical high-pressure belt over the Saharan territories.

Zonal and meridional wind components at 700 hPa define the main dust transport patterns with a relatively long west-east directional first phase dominated by zonal winds and northward transport over the Western Mediterranean basins toward Central Europe by a more enhanced meridional flow contribution (Fig. 3).

More than two-thirds (67.4%, n = 147; see Fig. 4. and Table 1.) of the identified SDEs were classified as Type-1 episodes. In the previous study by Varga et al. (2013) 66.2% of the total SDEs belonged to this synoptic group. Because of the large number of Type-1 events, the annual number of these episodes varied similarly to the total number of SDEs. The seasonal distribution of events of this synoptic group also showed the general spring-summer main phase. Dust material was transported during Type-1 events over the Western Mediterranean basins from north-western African source areas.

Well-developed Mediterranean cyclones have been the main drivers of Type-2 events. Almost a quarter (24.8%, n = 54) of the SDEs were grouped into this type (nearly identical to the reported seasonal distributions of 25.4% by Varga et al. (2013)). The southerly flow associated with the warm winds on the foreside of the eastward-moving low-pressure systems is responsible for dust transport. Wind flow maps (Fig. 3) also show the dominance of meridional flows over zonal ones. The main transport routes of Type-2 episodes were concentrated on the Central Mediterranean Basins. Occasionally, dust material could also be transported from the Levant by south-easterly flows at 700 hPa. The main period of Type-2 events was in spring with a secondary maximum in winter (particularly in February).

Seventeen type-3 episodes (7.8% of total) were registered during the 40 year period. Varga et al. (2013) reported an 8.5% proportion of Type-3 of SDEs between 1979 and 2011. Anticyclonic flows of a high-pressure centre over north-western Africa and south-western Europe carry dust material from western parts of the Sahara northward along the coastline or over the eastern Atlantic to the higher latitudes, where the dominant westerlies define the eastward movement of the dust-laden air-masses toward Central Europe.

Similar general types of synoptic situations of the Mediterranean were reported by previous studies using objective classification methods (s-mode factor analysis, k-means cluster analysis, and empirical orthogonal function analysis). Western Mediterranean analyses of Salvador et al. (2014) and Schepanski et al. (2016) presented atmospheric patterns favouring dust transport to south-western Europe; among them, several clusters were similar to Type-1 SDEs. Gkikas et al. (2015) investigated the broader Mediterranean Basin, among the introduced six atmospheric circulation patterns and their seasonal distributions, which can be matched with Type-1 and Type-2 SDEs of this study. Type-3 SDEs were not discussed by these studies; however, these rare SDEs have not been affected by the Mediterranean Basin.

In our previous study (Varga et al., 2016), data of BSC-DREAM8b (Barcelona Supercomputing Center's Dust REgional Atmospheric Model) v1.0 and v2.0 dust models and the mineral dust model database was used to assess the deposited Saharan dust. These modelled values corrected by a few direct surface observations of published European measurement campaigns indicated an average annual dust deposition of 3.2–5.4 g m^{-2} in the Carpathian Basin (Varga et al., 2016). MERRA-2 modelled data of the present study showed a slightly lower annual mineral dust deposition in Central Europe (1.2–3.55 g m^{-2}), dominated by wet deposition (77–93% mass of the total). The temporal distribution of Saharan dust deposition coincides with the seasonal pattern of Type-2 events (Mediterranean cyclones bring precipitation to Central Europe) by a dominant spring maximum with relatively high values in autumn and in February (especially from 2003, see Fig. 4).

Interannual changes of the number of SDEs and deposited dust material in the Carpathian Basin are obvious; however, no direct relationship among these frequencies and other climatic parameters (annual mean temperature, precipitation, and North Atlantic Oscillation phases) could be revealed. There is no general trend in the number of identified events; however, an increase in the annual occurrences in the last decade is rather apparent. In addition, the seasonal distribution of deposition changed in the last quarter of the studied period, and almost 25% of the Saharan dust deposition occurred during winter (Table 1).

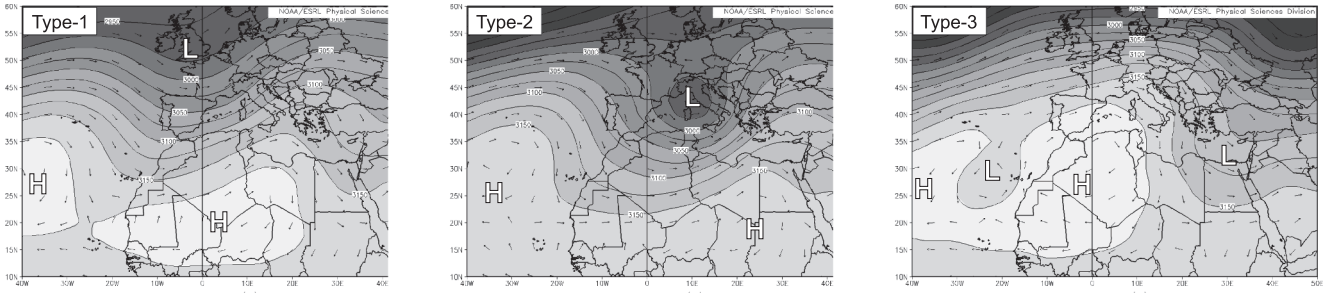

Fig. 2. Synoptic meteorological background (mean geopotential height map and wind vectors at 700 hPa) of different types of Saharan dust events.

3.2. Intense dust deposition events

Several considerably intense Saharan dust depositional events (SDDEs) were recorded after 2014. These were identified based on reported surface observations of mineral dust washout situations from the study area. An exceptionally large amount of mineral dust material was washed out during these episodes, which also attracted the attention of local society and (social) media. All of these SDDEs occurred between the end of October and February; before 2009, these episodes could be regarded as unseasonal episodes (Fig. 5).

3.2.1. SDDE #1: 19–20 February 2014

An intense unseasonal washout of Saharan dust occurred on 19–20 February 2014. A cut-off low (a small, closed depression) was left by an upper-level atmospheric trough, associated with a remarkable southerly meander of the jet stream leading to rain, snow, and dust storms in western Africa and Morocco on 16 February. Simultaneously with the north-eastward movement of the low-pressure system, its frontal winds injected a large amount of dust from the Algerian and Tunisian source areas into the atmosphere. An extensive high-pressure centre over Libya and Egypt blocked the eastward spread of the depression, and consequently, the dust-laden air mass was forced to follow a southwest-northeast flow and reached Central Europe on 19 February.

3.2.2. SDDE #2: 30 November – 1 December 2014

Synoptic backgrounds of the episode of November 2014 were also dominated by a cut-off low stemming from an atmospheric trough centred over south-western Europe and north-western Africa. A large

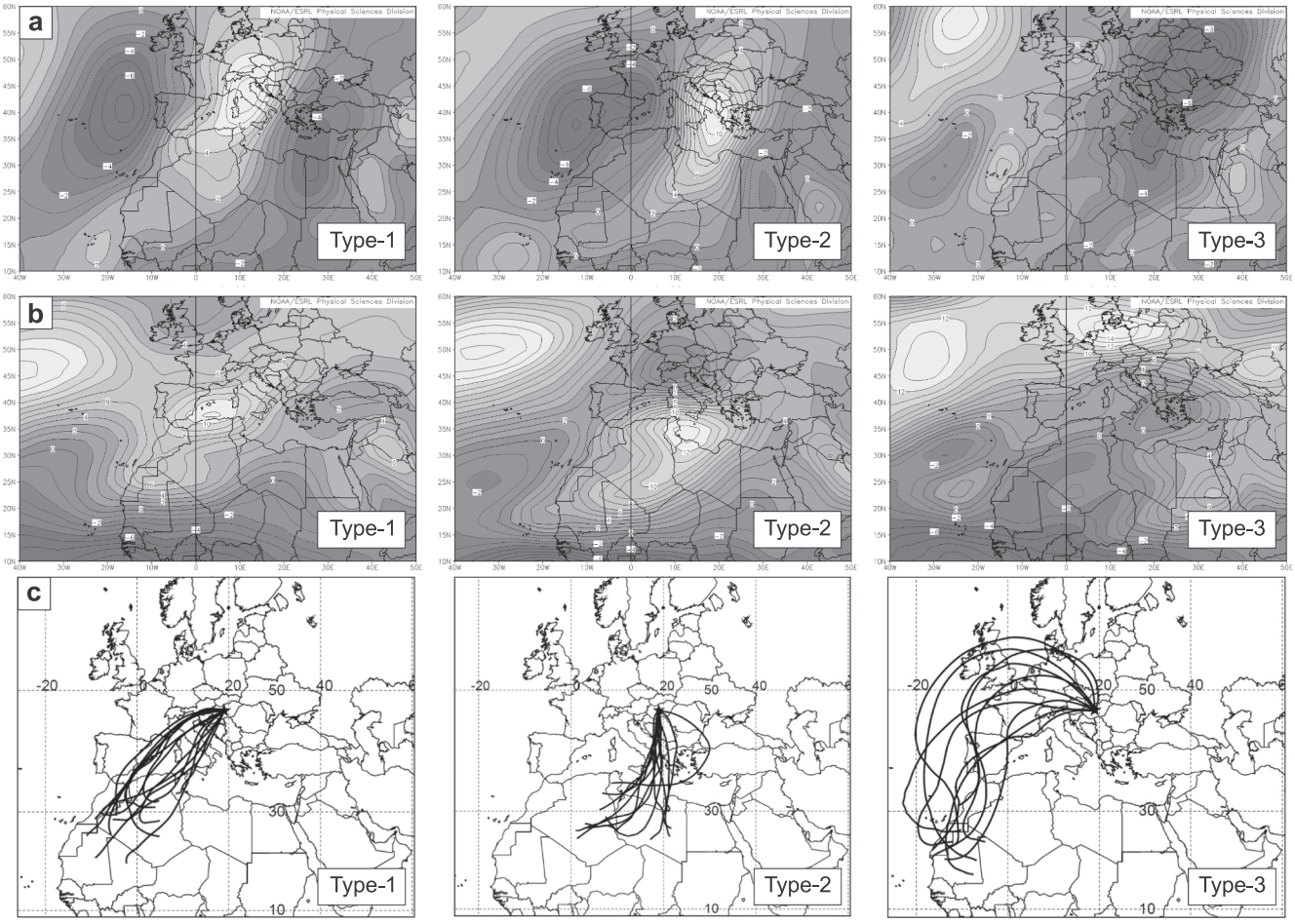

Fig. 3. Wind flow patterns (mean meridional (a) and zonal (b) wind components at 700 hPa) and specific dust transport routes at 3000 m a.s.l. by different Saharan dust event types.

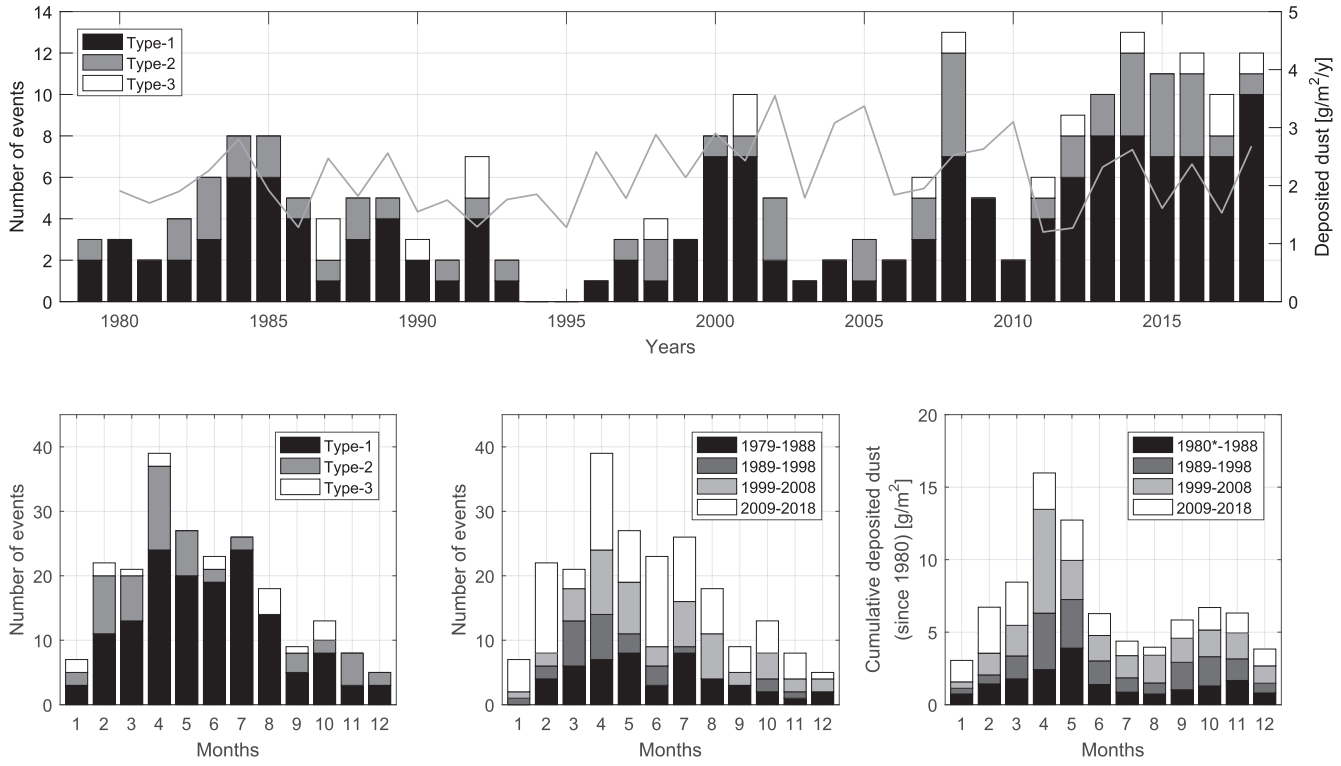

Fig. 4. Annual and monthly frequencies and deposition rates of Saharan dust events.

Table 1
Decadal changes of Saharan dust episodes and dust deposition.

Decade	SDEs				Deposition [g/m^2]								
	Events	Type-1	Type-2	Type-3	DJF	MAM	JJA	SON	Annual	DJF	MAM	JJA	SON
1979–1988	48	32(66.7%)	14(29.2%)	2(4.2%)	6(12.5%)	21(43.8%)	15(31.3%)	15(12.5%)	2.1	0.3(15.8%)	1.0(47.1%)	0.3(16.6%)	0.4(20.6%)
1989–1998	27	16(59.3%)	7(25.9%)	4(14.8%)	3(11.1%)	17(63.0%)	4(14.8%)	3(11.1%)	1.9	0.2(8.3%)	0.8(43.8%)	0.4(18.5%)	0.6(29.4%)
1999–2008	53	35(66.0%)	14(26.4%)	4(7.6%)	4(8.2%)	20(40.8%)	17(34.7%)	8(16.3%)	2.6	0.4(15.9%)	1.2(44.9%)	0.5(18.7%)	0.5(20.5%)
2009–2018	90	64(71.1%)	19(21.1%)	7(7.8%)	16(18.8%)	26(30.6%)	30(35.3%)	13(15.3%)	2.1	0.5(24.9%)	0.8(40.0%)	0.3(15.0%)	0.4(20.0%)
Full period	218	147(67.4%)	54(24.8%)	17(7.8%)	29(13.9%)	84(40.2%)	66(31.6%)	30(14.4%)	2.2	0.3(16.2%)	1.0(44.1%)	0.4(17.3%)	0.5(22.4%)

amount of Saharan mineral dust material was transported north-eastward by the prevailing south-western flow on the warm sector of the cyclone. Warm advection at 1000–2500 m a.s.l. associated with this dust event (and its convergence with the Siberian air-masses) caused freezing rain and sleet at high-altitude areas of Hungarian central regions and led to severe forest damage and destruction of power transmission lines.

3.2.3. SDDE #3: 22 February 2016

An intense dust storm caused severely reduced visibility conditions and a remarkable dust washout episode in the Iberian Peninsula on 21 February 2016 (Gama et al., 2019). The dust event was generated again by an atmospheric cut-off low separated from a deepened upper-level trough generated by the dust event. A large amount of the mineral dust was transported by the low-pressure system northward from salt lakes of the high plateau region situated between the Tell Atlas and Saharan Atlas Range, leading to an exceptionally intense wet deposition event on 23 February in Budapest, Hungary, where the deposited reddish-yellow dust material had blanketed parked cars and other exposed obstacles.

3.2.4. SDDE #4: 29 February 2016

Just a week later, on 29 February 2016, another unusually intense dust deposition event was observed in Budapest and was widespread in Hungary. A deep cyclone centred above the western basin of the Mediterranean Sea transported the yellowish dust material from Algerian, Tunisian, and Libyan source areas. The main dust transport route was over the Central Mediterranean.

3.2.5. SDDE #5: January 7–9, 2018

In the first days of 2018, an extensive cyclone developed from an upper-level trough over the Iberian Peninsula. The penetration of cold northerly air-mass caused intense snow in Algeria and resulted in a deep snow-cover in the region of Ain Sefra. The 700-hPa wind speed exceeded 25–30 m/s, and its dynamical forcing led to strong surface winds at the lee side of the Atlas Mountains, causing intense injection of mineral dust into the atmosphere. Warm sector winds of the cyclone transported the dust-laden air-masses towards Central Europe, where intense wet deposition was observed on January 9.

3.2.6. SDDE #6: 7–8 February 2018

A month later, on 5 February another cyclone was developed over the Iberian Peninsula from a trough emanating from north-western Europe. It was the second snow event within a month in Ain Sefra. Such an event has never been observed before. The strong cyclonal flow of the low-pressure system caused widespread dust storms at the foreside of the Atlas Mountains and around the Chott regions of Algeria and Tunisia. Dust material was transported northward over the Ionian and

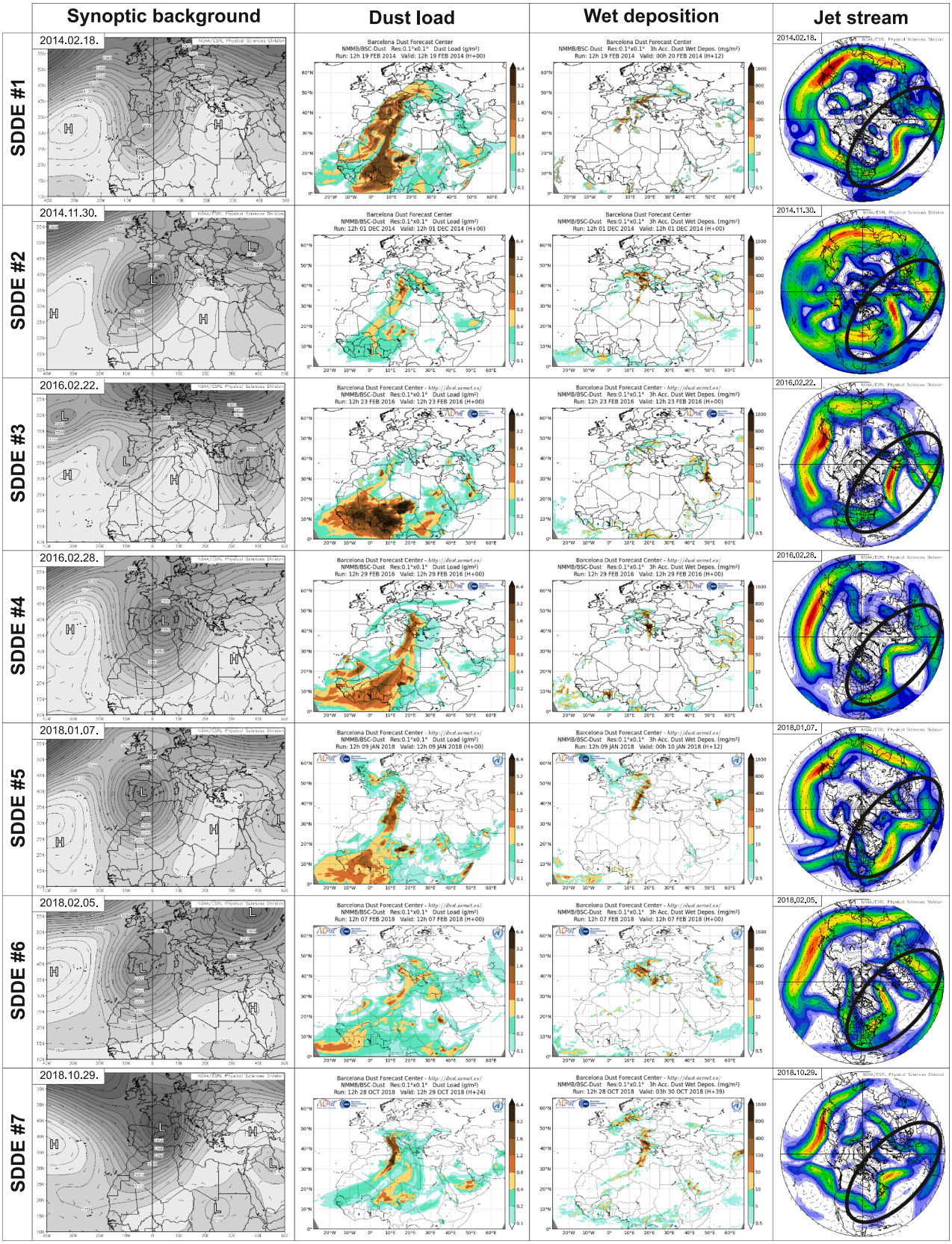

Fig. 5. General properties of the discussed intense Saharan dust depositional events (geopotential height and wind vectors at 700 hPa; modelled dust loading (NNMB/BSC); modelled wet deposition (NNMB/BSC); jet patterns (wind vectors at 200 hPa)).

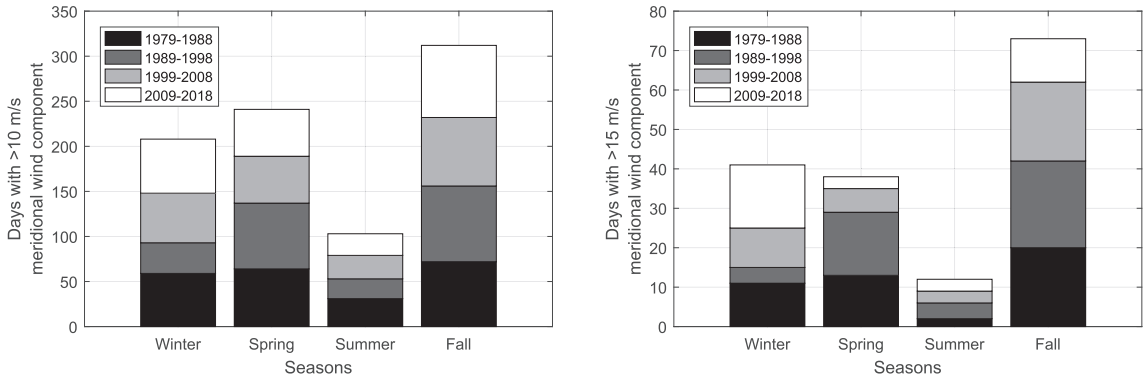

Fig. 6. Seasonal distribution of days with strong (> 10 m/s and > 15 m/s) meridional winds by decades.

Adriatic Seas to Central Europa and the Balkan Peninsula. The frontal system of the Mediterranean cyclone led to washout out of mineral particles on 7–8 February in Hungary.

3.2.7. SDDE #7: 28–29 October 2018

In the last days of October 2018, an extensive deep trough emanated from north-north-western Europe, resulting a very intense dust emission from the dust source areas located at the lee side of the Atlas Mountains. On October 28, the centre of the developed cyclone was located over the Gulf of Lion and the steep pressure gradient between the low-pressure system and the high-pressure area of Eastern Mediterranean led to a spectacular dust event over the central region of the Mediterranean, intensively affecting also Central Europe.

3.3. Meridional wind patterns

Seasonal intensity changes of meridional wind components were studied for the four investigated decades. The number and relative proportion of days when the speed of meridional wind components exceeded 10 and 15 m/s at 700 hPa showed dominance of fall in both cases, but more clearly for higher wind speeds (Fig. 6). Summers are represented by a relatively low number of such days, but springs and winters provide suitable conditions for gusty southerly atmospheric flow patterns. Decadal variability of days with enhanced (> 15 m/s) meridionality was rather significant, partly because of the low number of these days; however, the increased relative proportion in the winters of 2009–2018 (48.5% of the total decadal episodes) is remarkable.

3.4. Grain size of deposited dust material

The deposited mineral dust samples of the above presented SDDEs were characterised by particle size and shape analysis techniques using automated static image analysis and proved the presence of a larger volumetric proportion of medium (6.25–20.00 μm) and coarse silt-sized (20.00–62.50 μm) particles.

Occasionally, fine particles stacked on each other to form larger aggregates. This phenomenon was observed during the measurements of the samples of SDDE #1 (19–20 February 2014), when the laser diffraction measurements resulted a modal grain size of particle size distribution at 6.3 μm; however, images analysis results showed the clear presence of a larger quantity of coarse silt-sized aggregates, indicating that these Saharan minerals were not transported as individual fine-medium silt-sized particles. Large aggregates were accidentally dispersed during laser diffraction measurement, leading to the underestimated grain sizes. The dispersed grain sizes cannot be representative of the strength of the transport agent (e.g., wind speed); therefore, appropriate, non-destructive sizing technique should be chosen.

In other cases, a higher individual grain per aggregate ratio could be identified with a large proportion of single mineral grains (quartz, feldspar, calcium-carbonate, and dolomite) with a particle diameter over 30 μm (e.g., during SDDEs #2 and #3; 22 and 26 February 2016), and even larger ratios were observed during SDDE #6 on 7–8 February 2018. At this moment, because of the scarce homogeneous grain size data and general lack of grain shape data of Saharan dust source areas, source appointment cannot be performed solely based on granulometric data.

The published characteristic particle sizes of Saharan dust materials deposited in Europe are in the range of 2 to 30 μm. Particle size data (various single statistical descriptors were used) measured by different analytical techniques were taken from the compilation of Goudie and Middleton (2006): Crete: 8–30 μm (modal; Mattson and Nihlén, 1996), 4–16 μm (median); Spain: 4–30 μm (mean; Sala et al., 1996); Germany: 2.2–16 μm (median); Italy: 16.8 μm (modal), 14.6 μm (median; Ozer et al., 1998); South France: 4–12.7 μm (median; Bücher and Lucas, 1984), 8–11 μm (median; Coudé-Gaussen, 1991); France (Paris Basin): 8 μm (Coudé-Gaussen et al., 1988); Swiss Alps: 4.5 ± 1.5 μm (median; Wagenbach and Geis, 1989); and Central Mediterranean: 2–8 μm (modal; Tomadin et al., 1984). The identified Saharan quartz particles from the geological samples collected from Fuerteventura, Canary Islands (located significantly close to the African continent in the Atlantic Ocean, 100 km west of Morocco), showed ~ 70 μm modal and 68.5 μm median values (Varga and Roettig, 2018; Roettig et al., 2018).

3.5. Surface air temperature anomalies during the identified dust events

Enhanced southerly airflow patterns of SDEs also cause warm air advection in the mid-latitudes. Intrusions of dust-loaded North African air-masses into the Carpathian Basin caused an average warming of 3.5 °C compared to long-term (1981–2010) means. The mean decadal warm advection values of SDE-days showed an increasing trend from 2.3 °C in 1979–1988 to 4.0 °C in 2009–2018 (Table 2).

Zonal mean surface air temperature anomalies of peak SDE-days were calculated to show the seasonal and decadal meridional transect anomalies from 0° to 90°N latitudes (Fig. 7). The decadal temperature anomaly values clearly indicate the enhanced warming of high latitudes of the Northern hemisphere, whereas seasonal values show increased warming during winter and fall. Surface air temperature anomalies of 2009–2018 winter SDEs can be characterised by extremely high values of high latitudes of the Northern hemisphere. The enhanced warming of

Table 2
Seasonal surface air temperature anomalies of the SDE-days by decades.

Decades	Winter	Spring	Summer	Fall	Mean
1979–1988	3.7 °C	1.7 °C	2.6 °C	2.6 °C	2.3 °C
1989–1998	4.4 °C	2.8 °C	3.7 °C	4.4 °C	3.3 °C
1999–2008	3.7 °C	2.9 °C	4.6 °C	5.6 °C	3.9 °C
2009–2018	4.3 °C	3.0 °C	4.3 °C	4.9 °C	4.0 °C
Full period	4.4 °C	2.6 °C	4.0 °C	4.4 °C	3.5 °C

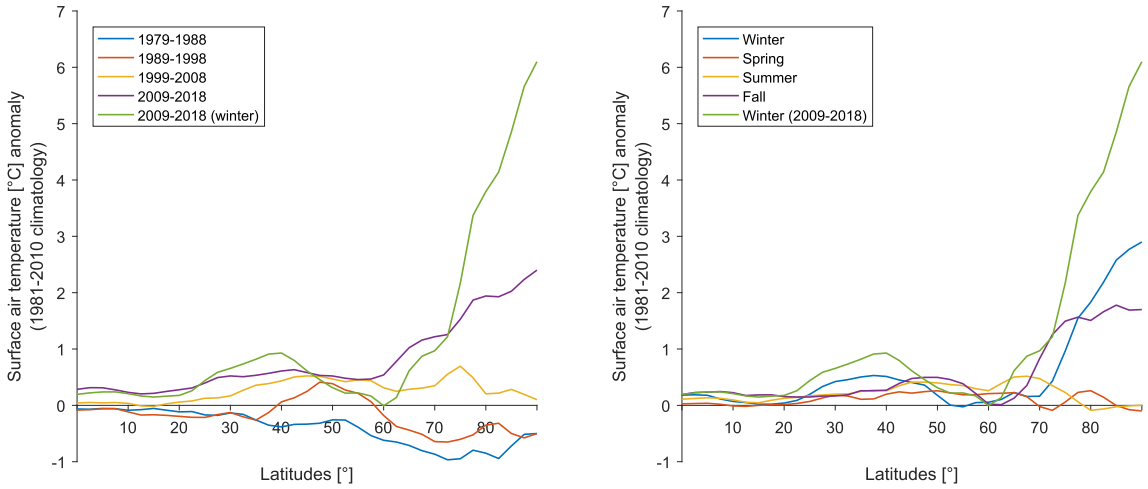

Fig. 7. Meridional transect (zonal mean) air temperature anomalies during the identified dust events by decade and by season.

high-latitude regions and the reduced temperature differences of the Arctic and lower latitude areas have an impact on other atmospheric processes. The meridional temperature gradient determines the strength of the jet stream partly and thus high-altitude flow patterns (e.g., the dominance of zonal or meridional winds).

4. Discussion

4.1. Wintertime dust events

All of the identified unusual dust events characterised by severe washout of mineral dust material in the Carpathian Basin were related to very similar synoptic meteorological situations. The first phase of the dust storm development was an enhanced southward propagation of a high-latitude upper-level atmospheric trough. The orographic blocking of Atlas Mountains played a vital role in the formation of sever surface wind storms and dust entrainment. According to Bou Karam et al. (2009), the low-level winds and dynamics are associated with the penetration of the atmospheric trough. The northward dust transport across the Mediterranean towards Central and south-eastern Europe was also related to the main flow patterns and the eastward-moving low-pressure system.

The occurrence and southerly penetration of high-latitude high-level atmospheric trough to low-latitudes and the increased meridionality of dominant flow patterns have been associated with the remarkable southerly meander of the jet stream, often associated with Arctic amplification (AA). AA is the enhanced warming of high-latitude regions compared to mid- and low-latitudes. AA along with its alternative metric, the difference in the 1000–500 hPa thickness change in the Arctic relative to that in mid-latitudes, is leading to more (less) meridional (zonal) flow at high altitudes and increasing planetary wave amplitudes (Francis and Vavrus, 2015).

Francis et al. (2018) identified the importance of more meandering polar jets in the Saharan cyclone formation and poleward mineral dust transport from North Africa. According to their findings, in winter, the dust storm formation at the lee side of Atlas Mountains is generated by high-latitude upper-level troughs and associated low-level dynamics, as well as meridional temperature gradient-driven development of Saharan cyclones (Francis et al., 2018). Therefore, the Saharan cyclone formation and poleward dust transport from Africa are affected by the increasing amplitude of planetary waves.

General airflow patterns of severe Saharan dust depositional events of the last decade in the Carpathian Basin, as well as increased frequency of gusty meridional flows and enhanced warming of high latitudes of Northern hemisphere, coincide. Thus, here, we confirm the findings of Francis et al. (2018), that the increasing occurrence of extreme Saharan dust events in Central Europe has been associated with enhanced warming of the Arctic, thereby leading to more meandering jet streams.

4.2. Grain size uncertainties-driven deposition data issues

The general increasing trend of numbers of SDEs and the increasing wintertime amount of deposited dust material should not necessarily correspond to the increasing intensity of dust events, and even the opposite can be concluded from the raw data. Intensification, however, was indicated by direct surface observations of intense dust washout episodes when the deposited reddish-yellow dust material had blanketed parking cars, roof-windows, and other exposed obstacles. Numerical simulations of dust deposition also revealed a wintertime increase of the number and magnitude of dust episodes. Nevertheless, the extent of it was not equivalent to the growth of the SDE numbers. A few previous studies confirmed the significant underestimation of deposited mineral dust material by numerical simulations. Quantitative values of valuable but scarce surface measurements and satellite-based assessments have been several orders of magnitudes larger than the modelling results, but the spatial and temporal (e.g., interannual, seasonal) patterns of dust deposition have been properly simulated by the dust models (Gallisai et al., 2014; Varga et al., 2016; Yu et al., 2019).

According to our suggestions, grain size should be the key to resolve this contradiction. Several recent papers reported the measurements of giant mineral particles found in far-travelled mineral dust (Betzer et al., 1998; Maring et al., 2003; Renard et al., 2018; van der Does et al., 2018). Our automated static image analyses of Saharan dust material in the Carpathian Basin also indicated that the grain size of transported Saharan dust material could be significantly larger than the grain sizes predicted by the model (Varga et al., 2016). Mineral grains > 20 μm are not parametrised in the numerical simulations. Mineral grains of > 20 μm are usually not accounted for in the numerical simulations (in the majority of global and regional dust models, only some size-bins of a relatively narrow size range are applied; Benedetti et al., 2014) (Fig. 8.). Because of the cubic relationship between particle diameter and volume (mass), even a small change in applied size-bins can lead to a significant increase of modelled dust fluxes. A deeper understanding of grain size-related uncertainties would also be useful to explore the relationship between uncertain granulometric parametrisation in retrieval algorithms of satellite observations and mineral dust flux estimations.

In addition, the physical background of long-range transport of such a giant mineral material is a matter of debate in the scientific literature (Betzer et al., 1988; Ryder et al., 2013; Weinzierl et al., 2017; Marenco et al., 2018; van der Does et al., 2018). This lack of understanding of

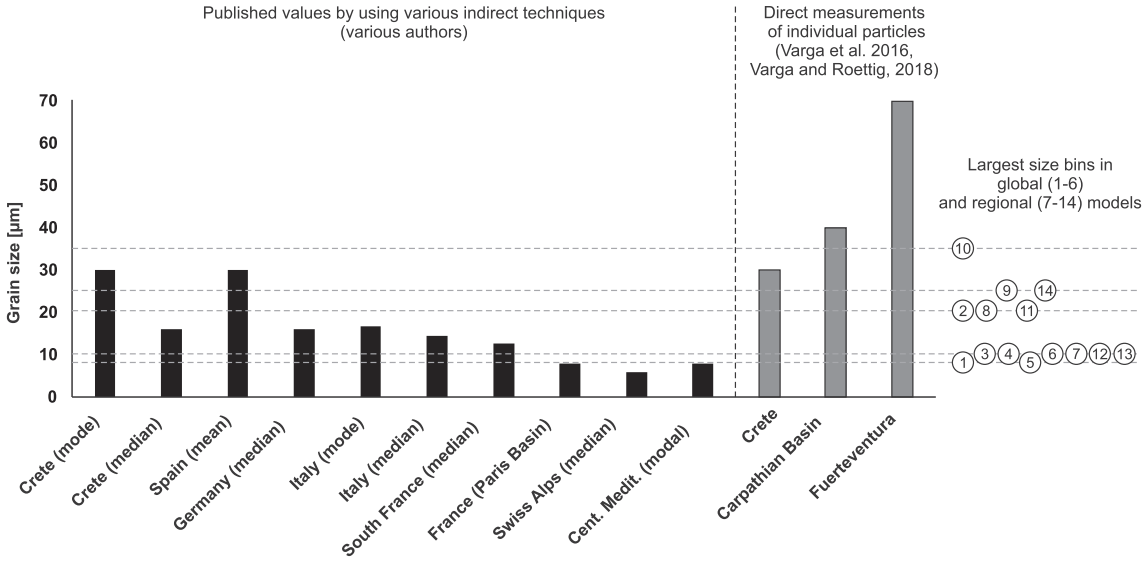

Fig. 8. Reported grain size values of Saharan dust in the Mediterranean (indicated models: 1: GEOS-5; 2: MACC_II; 3: MASINGAR; 4: MetUM; 6: NGAC; 7: NMMB/BSC-Dust; 8: CHIMERE; 9: CMAQ-KOSA; 10: COAMPS; 11: CUACE/Dust; 12: BSC-DREAM8b; 13: DREAM8-NMME-MACC; 14: TAQM_KOSA;).
Source: Benedetti et al., 2014

driving mechanisms makes the evaluation of radiative forcing of atmospheric mineral dust difficult because the net climate effect of dust (scattering and absorption) depends on grain size distribution; larger particles act like greenhouse gases by absorbing and emitting longwave radiation and have a heating effect, whereas fine dust cools the atmosphere (Otto et al., 2007, 2009).

5. Conclusions

The purpose of the current study was to present a long-term time series and systematic analysis of Saharan dust episodes identified in the Carpathian Basin and provide new information and an explanation on changing temporal patterns of dust events. SDEs of the last 40-years indicated the definite role of specific synoptic meteorological situations in the formation of North African dust transport toward Central Europe. Several intense episodes were recorded after 2014 when an exceptionally large amount of mineral dust material was washed out, and all occurred between the end of October and February, although the main period of dust transport to Europe is the spring and summer. Synoptic analyses confirmed that majority of the events were associated with very similar atmospheric patterns; generally, an upper-level atmospheric trough (the result of a remarkable meander of the jet stream) led to the development of a cut-off low over the north-east, which deepened the low-pressure system which transported large amounts of the mineral dust northward.

The presented individual events revealed the clearly changing characteristics of recent wintertime Saharan dust deposition episodes, increased number of days with gusty meridional flows at 700 hPa in winter, and enhanced warming of high latitudes of the Northern hemisphere during severe winter dust events of the last decade. Saharan cyclone formation and poleward dust transport from Africa are affected by the increasing amplitude of planetary waves. These extreme events can be linked to AA, which is the possible cause of the development of a more meandering jet stream (and wavy polar vortex) as a result of decreasing temperature differences of the Arctic and lower latitudes driven by the faster warming high latitudes.

CRediT authorship contribution statement

György Varga: Conceptualization, Data curation, Investigation, Methodology, Validation, Visualization, Writing - original draft, Writing - review & editing.

Declaration of Competing Interest

The authors declare that they have no known competing financial interests or personal relationships that could have appeared to influence the work reported in this paper.

Acknowledgement

Support by the National Research, Development and Innovation Office (NKFIH K120620 and KH130337) is gratefully acknowledged. The research was additionally supported by the MTA research fund KEP-08/2018. The author would like to acknowledge the COST Action inDust (COST Action CA16202).

References

Albrecht, B.A., 1989. Aerosols, cloud microphysics, and fractional cloudiness. Science (80). 245, 1227–1230. https://doi.org/10.1126/science.245.4923.1227.
Alpert, P., Kishcha, P., Shtivelman, A., Krichak, S.O., Joseph, J.H., 2004. Vertical distribution of Saharan dust based on 2.5-year model predictions. Atmos. Res. 70 (2), 109–130. https://doi.org/10.1016/j.atmosres.2003.11.001.
Amiridis, V., Wandinger, U., Marinou, E., Giannakaki, E., Tsekeri, A., Basart, S., Kazadzis, S., Gkikas, A., Taylor, M., Baldasano, J., Ansmann, A., 2013. Optimizing CALIPSO Saharan dust retrievals. Atmos. Chem. Phys. 13, 12089–12106. https://doi.org/10.5194/acp-13-12089-2013.
Atalay, I., 1997. Red Mediterranean soils in some karstic regions of Taurus mountains, Turkey. Catena 28, 247–260. https://doi.org/10.1016/S0341-8162(96)00041-0.
Bangert, M., Nenes, A., Vogel, B., Vogel, H., Barahona, D., Karydis, V.A., Kumar, P., Kottmeier, C., Blahak, U., 2012. Saharan dust event impacts on cloud formation and radiation over Western Europe. Atmos. Chem. Phys. 12, 4045–4063. https://doi.org/10.5194/acp-12-4045-2012.
Barkan, J., Alpert, P., 2010. Synoptic analysis of a rare event of Saharan dust reaching the Arctic region. Weather 65 (8), 208–211. https://doi.org/10.1002/wea.503.
Barkan, J., 2005. Synoptics of dust transport days from Africa toward Italy and central Europe. J. Geophys. Res. 110 (D7), D07208. https://doi.org/10.1029/2004JD005222.
Basart, S., Pérez, C., Nickovic, S., Cuevas, E., Baldasano, J., 2012. Development and evaluation of the BSC-DREAM8b dust regional model over Northern Africa, the Mediterranean and the Middle East. Tellus B Chem. Phys. Meteorol. 64 (1), 18539. https://doi.org/10.3402/tellusb.v64i0.18539.
Benedetti, A., J.M. Baldasano, S. Basart, F. Benincasa, O. Boucher, M.E. Brooks, J.-P. Chen, P.R. Colarco, S. Gong, N. Huneeus, L. Jones, S. Lu, L. Menut, J.-J. Morcrette, J. Mulcahy, S. Nickovic, C. Pérez García-Pando, J.S. Reid, T.T. Sekiyama, T.Y. Tanaka, E. Terradellas, D.L. Westphal, X.-Y. Zhang, and C.-H. Zhou: Operational dust prediction. In Mineral Dust: A Key Player in the Earth System. P. Knippertz and J.-B.W. Stuut, Eds. Springer, pp. 223-265, Doi:10.1007/978-94-017-8978-3_10, 2014.
Betzer, P.R., Carder, K.L., Duce, R.A., Merrill, J.T., Tindale, N.W., Uematsu, M., Costello, D.K., Young, R.W., Feely, R.A., Breland, J.A., Bernstein, R.E., Greco, A.M., 1988. Long-range transport of giant mineral aerosol particles. Nature 336 (6199), 568–571.

https://doi.org/10.1038/336568a0.
Borbély-Kiss, I., Kiss, Á.Z., Koltay, E., Szabó, G., Bozó, L., 2004. Saharan dust episodes in Hungarian aerosol: Elemental signatures and transport trajectories. J. Aerosol Sci. 35 (10), 1205–1224. https://doi.org/10.1016/j.jaerosci.2004.05.001.
Boucher, O. et al. in Climate Change: The Physical Science Basis. Contribution of Working Group I to the Fifth Assessment Report of the Intergovernmental Panel on Climate Change (Stocker, T. F. et al., eds). 571–657 (Cambridge Univ. Press, 2013), doi:10.1017/CBO9781107415324, 2013.
Bücher, A., Lucas, G., 1984. Sédimentation éolienne intercontinentale, poussières sahariennes et géologie. Bull. Cent. Rech. Elf. E. 8, 151–165.
Burt, S., 1991. Falls of dust rain within the British Isles. Weather 46 (11), 347–353. https://doi.org/10.1002/j.1477-8696.1991.tb07075.x.
Coudé-Gaussen, G., Désiré, E., Regrain, R., 1988. Particularité de poussières sahariennes distales tombées sur la Picardie et l'Ile-de-France le 7 Mai 1988. Hommes Terr. 4, 246–251.
Coudé-Gaussen, G.: Les poussières sahariennes: cycle sédimentaire et place dans les environments et paléoenvironments désertiques. Montrouge: John Libby Eurotext, 485 pp., 1991.
Di Biagio, C., di Sarra, A., Meloni, D., Monteleone, F., Piacentino, S., Sferlazzo, D., 2009. Measurements of Mediterranean aerosol radiative forcing and influence of the single scattering albedo. J. Geophys. Res. 114, D06211. https://doi.org/10.1029/2008JD011037.
Di Mauro, B., Fava, F., Ferrero, L., Garzonio, R., Baccolo, G., Delmonte, B., Colombo, R., 2015. Mineral dust impact on snow radiative properties in the European Alps combining ground, UAV, and satellite observations. J. Geophys. Res. Atmos. 120, 6080–6097. https://doi.org/10.1002/2015JD023287.
Di Mauro, B., Garzonio, R., Rossini, M., Filippa, G., Pogliotti, P., Galvagno, M., Morra di Cella, U., Migliavacca, M., Baccolo, G., Clemenza, M., Delmonte, B., Maggi, V., Dumont, M., Tuzet, F., Lafaysse, M., Morin, S., Cremonese, E., Colombo, R., 2019. Saharan dust events in the European Alps: role in snowmelt and geochemical characterization. Cryosph. 13, 1147–1165. https://doi.org/10.5194/tc-13-1147-2019.
Di Tomaso, E., Schutgens, N.A.J., Jorba, O., Pérez García-Pando, C., 2017. Assimilation of MODIS Dark Target and Deep Blue observations in the dust aerosol component of NMMB-MONARCH version 1.0. Geosci. Model Dev. 10, 1107–1129. https://doi.org/10.5194/gmd-10-1107-2017.
Drake, J.J., 1981. The Effects of Surface Dust on Snowmelt Rates. Arct. Alp. Res. 13, 219. https://doi.org/10.2307/1551197.
Dulac, F., Tanré, D., Bergametti, G., Buat-Ménard, P., Desbois, M., Sutton, D., 1992. Assessment of the African airborne dust mass over the western Mediterranean Sea using Meteosat data. J. Geophys. Res. 97 (D2), 2489. https://doi.org/10.1029/91JD02427.
Durn, G., Ottner, F., Slovenec, D., 1999. Mineralogical and geochemical indicators of the polygenetic nature of terra rossa in Istria, Croatia. Geoderma 91, 125–150. https://doi.org/10.1016/S0016-7061(98)00130-X.
Fan, S.-M., Moxim, W.J., Levy II, H., 2006. Aeolian input of bioavailable iron to the ocean. Geophys. Res. Lett. 33. https://doi.org/10.1029/2005GL024852.
Francis, D., Eayrs, C., Chaboureau, J., Mote, T., Holland, D.M., 2018. Polar Jet Associated Circulation Triggered a Saharan Cyclone and Derived the Poleward Transport of the African Dust Generated by the Cyclone. J. Geophys. Res. Atmos. 123 (21), 11899–11917. https://doi.org/10.1029/2018JD029095.
Francis, J.A., Vavrus, S.J., 2015. Evidence for a wavier jet stream in response to rapid Arctic warming. Environ. Res. Lett. 10 (1), 014005. https://doi.org/10.1088/1748-9326/10/1/014005.
Franzén, L.G., Hjelmroos, M., Kållberg, P., Brorström-Lunden, E., Juntto, S., Savolainen, A.L., 1994. The "yellow snowepisode" of northern Fennoscandia, March 1991-A case study of long-distance transport of soil, pollen and stable organic compounds. Atmos. Environ. 28 (22), 3587–3604. https://doi.org/10.1016/1352-2310(94)00191-M.
Gallisai, R., Peters, F., Volpe, G., Basart, S., Baldasano, J.M., 2014. Saharan dust deposition may affect phytoplankton growth in the mediterranean sea at ecological time scales. PLoS One 9 (10), 110762. https://doi.org/10.1371/journal.pone.0110762.
Gama, C., Ribeiro, I., Lange, A.C., Vogel, A., Ascenso, A., Seixas, V., Elbern, H., Borrego, C., Friese, E., Monteiro, A., 2019. Performance assessment of CHIMERE and EURAD-IM' dust modules. Atmos. Pollut. Res. 10, 1336–1346. https://doi.org/10.1016/j.apr.2019.03.005.
Gao, H., Washington, R., 2009. The spatial and temporal characteristics of TOMS AI over the Tarim Basin, China. Atmos. Environ. 43 (5), 1106–1115. https://doi.org/10.1016/j.atmosenv.2008.11.013.
Gassó, S., Torres, O., 2019. Temporal characterization of dust activity in the Central Patagonia Desert (Years 1964–2017). J. Geophys. Res. Atmos. 124, 3417–3434. https://doi.org/10.1029/2018JD030209.
Gelaro, R., McCarty, W., Suárez, M.J., Todling, R., Molod, A., Takacs, L., Randles, C.A., Darmenov, A., Bosilovich, M.G., Reichle, R., Wargan, K., Coy, L., Cullather, R., Draper, C., Akella, S., Buchard, V., Conaty, A., da Silva, A.M., Gu, W., Kim, G.K., Koster, R., Lucchesi, R., Merkova, D., Nielsen, J.E., Partyka, G., Pawson, S., Putman, W., Rienecker, M., Schubert, S.D., Sienkiewicz, M., Zhao, B., 2017. The modern-era retrospective analysis for research and applications, version 2 (MERRA-2). J. Clim. 30 (14), 5419–5454. https://doi.org/10.1175/JCLI-D-16-0758.1.
Gerasopoulos, E., Kouvarakis, G., Babasakalis, P., Vrekoussis, M., Putaud, J.P., Mihalopoulos, N., 2006. Origin and variability of particulate matter (PM10) mass concentrations over the Eastern Mediterranean. Atmos. Environ. 40 (25), 4679–4690. https://doi.org/10.1016/j.atmosenv.2006.04.020.
Ginoux, P., 2017. Atmospheric chemistry: Warming or cooling dust? Nat. Geosci. 10, 246–248. https://doi.org/10.1038/ngeo2923.
Gkikas, A., Hatzianastassiou, N., Mihalopoulos, N., 2009. Aerosol events in the broader Mediterranean basin based on 7-year (2000–2007) MODIS C005 data. Ann. Geophys. 27 (9), 3509–3522. https://doi.org/10.5194/angeo-27-3509-2009.
Gkikas, A., Hatzianastassiou, N., Mihalopoulos, N., Katsoulis, V., Kazadzis, S., Pey, J., Querol, X., Torres, O., 2013. The regime of intense desert dust episodes in the Mediterranean based on contemporary satellite observations and ground measurements. Atmos. Chem. Phys. 13 (23), 12135–12154. https://doi.org/10.5194/acp-13-12135-2013.
Gkikas, A., Houssos, E.E., Lolis, C.J., Bartzokas, A., Mihalopoulos, N., Hatzianastassiou, N., 2015. Atmospheric circulation evolution related to desert-dust episodes over the Mediterranean. Q. J. R. Meteorol. Soc. 141, 1634–1645. https://doi.org/10.1002/qj.2466.
Ginoux, P., Chin, M., Tegen, I., Prospero, J.M., Holben, B., Dubovik, O., Lin, S.-J., 2001. Sources and distributions of dust aerosols simulated with the GOCART model. J. Geophys. Res. Atmos. 106, 20255–20273. https://doi.org/10.1029/2000JD000053.
Gkikas, A., Basart, S., Hatzianastassiou, N., Marinou, E., Amiridis, V., Kazadzis, S., Pey, J., Querol, X., Jorba, O., Gasso, S., Baldasano, J.M., 2016. Mediterranean intense desert dust outbreaks and their vertical structure based on remote sensing data. Atmos. Chem. Phys. 16 (13), 8609–8642. https://doi.org/10.5194/acp-16-8609-2016.
Gkikas, A., Obiso, V., Pérez García-Pando, C., Jorba, O., Hatzianastassiou, N., Vendrell, L., Basart, S., Solomos, S., Gassó, S., Baldasano, J.M., 2018. Direct radiative effects during intense Mediterranean desert dust outbreaks. Atmos. Chem. Phys. 18, 8757–8787. https://doi.org/10.5194/acp-18-8757-2018.
Gkikas, A., Giannaros, T.M., Kotroni, V., Lagouvardos, K., 2019. Assessing the radiative impacts of an extreme desert dust outbreak and the potential improvements on short-term weather forecasts: The case of February 2015. Atmos. Res. 226, 152–170. https://doi.org/10.1016/j.atmosres.2019.04.020.
Greilinger, M., Schauer, G., Baumann-Stanzer, K., Skomorowski, P., Schöner, W., Kasper-Giebl, A., 2018. Contribution of Saharan Dust to Ion Deposition Loads of High Alpine Snow Packs in Austria (1987–2017). Front. Earth Sci. 6. https://doi.org/10.3389/feart.2018.00126.
Haustein, K., Pérez, C., Baldasano, J.M., Jorba, O., Basart, S., Miller, R.L., Janjic, Z., Black, T., Nickovic, S., Todd, M.C., Washington, R., Müller, D., Tesche, M., Weinzierl, B., Esselborn, M., Schladitz, A., 2012. Atmospheric dust modeling from meso to global scales with the online NMMB/BSC-Dust model – Part 2: Experimental campaigns in Northern Africa. Atmos. Chem. Phys. 12, 2933–2958. https://doi.org/10.5194/acp-12-2933-2012.
Haustein, K., Pérez, C., Baldasano, J.M., Müller, D., Tesche, M., Schladitz, A., Esselborn, M., Weinzierl, B., Kandler, K., Von Hoyningen-Huene, W., 2009. Regional dust model performance during SAMUM 2006. Geophys. Res. Lett. 36, n/a-n/a. https://doi.org/10.1029/2008GL036463.
Herman, J.R., Bhartia, P.K., Torres, O., Hsu, C., Seftor, C., Celarier, E., 1997. Global distribution of UV-absorbing aerosols from Nimbus 7/TOMS data. J. Geophys. Res. Atmos. 102 (14), 16911–16922. https://doi.org/10.1029/96jd03680.
Huang, J., Wang, T., Wang, W., Li, Z., and Yan, H. (2014), Climate effects of dust aerosols over East Asian arid and semiarid regions, J. Geophys. Res. Atmos., 119, 11,398– 11, 416, Doi: 10.1002/2014JD021796.
Husar, R.B., Prospero, J.M., Stowe, L.L., 1997. Characterization of tropospheric aerosols over the oceans with the NOAA advanced very high resolution radiometer optical thickness operational product. J. Geophys. Res. Atmos. 102 (14), 16889–16909. https://doi.org/10.1029/96jd04009.
Israelevich, P. L., Levin, Z., Joseph, J. H. and Ganor, E.: Desert aerosol transport in the Mediterranean region as inferred from the TOMS aerosol index, J. Geophys. Res. Atmos., 107(D21), AAC 13-1-AAC 13-13, Doi:10.1029/2001JD002011, 2002.
Kalnay, E., Kanamitsu, M., Kistler, R., Collins, W., Deaven, D., Gandin, L., Iredell, M., Saha, S., White, G., Woollen, J., Zhu, Y., Chelliah, M., Ebisuzaki, W., Higgins, W., Janowiak, J., Mo, K.C., Ropelewski, C., Wang, J., Leetmaa, A., Reynolds, R., Jenne, R., Joseph, D., 1996. The NCEP/NCAR 40-year reanalysis project. Bull. Am. Meteorol. Soc. 77 (3), 437–471. https://doi.org/10.1175/1520-0477(1996)077<0437:TNYRP>2.0.CO;2.
Kis, A., Pongrácz, R., Bartholy, J., 2017. Multi-model analysis of regional dry and wet conditions for the Carpathian Region. Int. J. Climatol. 37, 4543–4560. https://doi.org/10.1002/joc.5104.
Klein, H., Nickovic, S., Haunold, W., Bundke, U., Nillius, B., Ebert, M., Weinbruch, S., Schuetz, L., Levin, Z., Barrie, L.A., Bingemer, H., 2010. Saharan dust and ice nuclei over Central Europe. Atmos. Chem. Phys. 10, 10211–10221. https://doi.org/10.5194/acp-10-10211-2010.
Koltay, E., Borbély-Kiss, I., Kertész, Z., Kiss, Á.Z., Szabó, G., 2006. Assignment of Saharan dust sources to episodes in Hungarian atmosphere by PIXE and TOMS observations. J. Radioanal. Nucl. Chem. 267 (2), 449–459. https://doi.org/10.1007/s10967-006-0073-1.
Marenco, F., Ryder, C., Estellés, V., O'Sullivan, D., Brooke, J., Orgill, L., Lloyd, G. and Gallagher, M.: Unexpected vertical structure of the Saharan Air Layer and giant dust particles during AER-D, Atmos. Chem. Phys., 18(23), 17655–17668, Doi:10.5194/acp-18-17655-2018, 2018.
MacLeod, D.A., 1980. The origin of the red Mediterranean soils in Epirus, Greece. J. Soil Sci. 31, 125–136. https://doi.org/10.1111/j.1365-2389.1980.tb02070.x.
Maring, H., Savoie, D.L., Izaguirre, M.A., Custals, L., Reid, J.S., 2003. Mineral dust aerosol size distribution change during atmospheric transport. J. Geophys. Res. D Atmos. 108 (19). https://doi.org/10.1029/2002jd002536.
Matassoni, L., Pratesi, G., Centioli, D., Cadoni, F., Lucarelli, F., Nava, S., Malesani, P., 2011. Saharan dust contribution to PM 10, PM 2.5 and PM 1 in urban and suburban areas of Rome: A comparison between single-particle SEM-EDS analysis and whole-sample PIXE analysis. J. Environ. Monit. 13 (3), 732–742. https://doi.org/10.1039/c0em00535e.
Meskhidze, N., Chameides, W.L., Nenes, A., 2005. Dust and pollution: A recipe for enhanced ocean fertilization? J. Geophys. Res. D Atmos. 110, 1–23. https://doi.org/10.1029/2004JD005082.
Mona, L., Amodeo, A., Pandolfi, M., Pappalardo, G., 2006. Saharan dust intrusions in the

Mediterranean area: Three years of Raman lidar measurements. J. Geophys. Res. Atmos. 111. https://doi.org/10.1029/2005JD006569.
Moulin, C., Lambert, C.E., Dayan, U., Masson, V., Ramonet, M., Bousquet, P., Legrand, M., Balkanski, Y.J., Guelle, W., Marticorena, B., Bergametti, G., Dulac, F., 1998. Satellite climatology of African dust transport in the Mediterranean atmosphere. J. Geophys. Res. Atmos. 103 (D11), 13137–13144. https://doi.org/10.1029/98JD00171.
Muhs, D.R., Budahn, J., Avila, A., Skipp, G., Freeman, J., Patterson, D.A., 2010. The role of African dust in the formation of Quaternary soils on Mallorca, Spain and implications for the genesis of Red Mediterranean soils. Quat. Sci. Rev. 29, 2518–2543. https://doi.org/10.1016/j.quascirev.2010.04.013.
Nabat, P., Somot, S., Mallet, M., Michou, M., Sevault, F., Driouech, F., Meloni, D., di Sarra, A., Di Biagio, C., Formenti, P., Sicard, M., Léon, J.-F., Bouin, M.-N., 2015. Dust aerosol radiative effects during summer 2012 simulated with a coupled regional aerosol–atmosphere–ocean model over the Mediterranean. Atmos. Chem. Phys. 15, 3303–3326. https://doi.org/10.5194/acp-15-3303-2015.
Otto, S., Bierwirth, E., Weinzierl, B., Kandler, K., Esselborn, M., Tesche, M., Schladitz, A., Wendisch, M., Trautmann, T., 2009. Solar radiative effects of a Saharan dust plume observed during SAMUM assuming spheroidal model particles. Tellus B Chem. Phys. Meteorol. 61 (1), 270–296. https://doi.org/10.1111/j.1600-0889.2008.00389.x.
Otto, S., de Reus, M., Trautmann, T., Thomas, A., Wendisch, M., Borrmann, S., 2007. Atmospheric radiative effects of an in situ measured Saharan dust plume and the role of large particles. Atmos. Chem. Phys. 7 (18), 4887–4903. https://doi.org/10.5194/acp-7-4887-2007.
Pandolfi, M., Tobias, A., Alastuey, A., Sunyer, J., Schwartz, J., Lorente, J., Pey, J., Querol, X., 2014. Effect of atmospheric mixing layer depth variations on urban air quality and daily mortality during Saharan dust outbreaks. Sci. Total Environ. 494–495, 283–289. https://doi.org/10.1016/j.scitotenv.2014.07.004.
Papayannis, A., Amiridis, V., Mona, L., Tsaknakis, G., Balis, D., Bösenberg, J., Chaikovski, A., De Tomasi, F., Grigorov, I., Mattis, I., Mitev, V., Müller, D., Nickovic, S., Pérez, C., Pietruczuk, A., Pisani, G., Ravetta, F., Rizi, V., Sicard, M., Trickl, T., Wiegner, M., Gerding, M., Mamouri, R.E., D'Amico, G., Pappalardo, G., 2008. Systematic lidar observations of Saharan dust over Europe in the frame of EARLINET (2000–2002). J. Geophys. Res. 113 (D10), D10204. https://doi.org/10.1029/2007JD009028.
Penner, J.E., 2019. Soot, sulfate, dust and the climate — three ways through the fog. Nature 570 (7760), 158–159. https://doi.org/10.1038/d41586-019-01791-6.
Pérez, C., Nickovic, S., Baldasano, J.M., Sicard, M., Rocadenbosch, F., Cachorro, V.E., 2006a. A long Saharan dust event over the western Mediterranean: Lidar, Sun photometer observations, and regional dust modeling. J. Geophys. Res. 111 (D15), D15214. https://doi.org/10.1029/2005JD006579.
Pérez, C., Nickovic, S., Pejanovic, G., Baldasano, J.M., Özsoy, E., 2006b. Interactive dust-radiation modeling: A step to improve weather forecasts. J. Geophys. Res. 111 (D16), D16206. https://doi.org/10.1029/2005JD006717.
Pérez, C., Haustein, K., Janjic, Z., Jorba, O., Huneeus, N., Baldasano, J.M., Black, T., Basart, S., Nickovic, S., Miller, R.L., Perlwitz, J.P., Schulz, M., Thomson, M., 2011. Atmospheric dust modeling from meso to global scales with the online NMMB/BSC-Dust model – Part 1: Model description, annual simulations and evaluation. Atmos. Chem. Phys. 11, 13001–13027. https://doi.org/10.5194/acp-11-13001-2011.
Perez, L., Tobias, A., Querol, X., Küzli, N., Pey, J., Alastuey, A., Viana, M., Valero, N., González-Cabré, M., Sunyer, J., 2008. Coarse particles from saharan dust and daily mortality. Epidemiology 19 (6), 800–807. https://doi.org/10.1097/EDE.0b013e31818131cf.
Pey, J., Querol, X., Alastuey, A., Forastiere, F., Stafoggia, M., 2013. African dust outbreaks over the Mediterranean Basin during 2001–2011: PM10 concentrations, phenomenology and trends, and its relation with synoptic and mesoscale meteorology. Atmos. Chem. Phys. 13 (3), 1395–1410. https://doi.org/10.5194/acp-13-1395-2013.
Prospero, J.M., Ginoux, P., Torres, O., Nicholson, S.E., Gill, T.E., 2002. Environmental characterization of global sources of atmospheric soil dust identified with the NIMBUS 7 Total Ozone Mapping Spectrometer (TOMS) absorbing aerosol product. Rev. Geophys. 40, 1002. https://doi.org/10.1029/2000RG000095.
Psenner, R., 1999. Living in a dusty world: airborne dust as a key factor for alpine lakes. Water. Air. Soil Pollut. https://doi.org/10.1023/A:1005082832499.
Querol, X., Alastuey, A., Pey, J., Cusack, M., Pérez, N., Mihalopoulos, N., Theodosi, C., Gerasopoulos, E., Kubilay, N., Koçak, M., 2009. Variability in regional background aerosols within the Mediterranean. Atmos. Chem. Phys. 9, 4575–4591. https://doi.org/10.5194/acp-9-4575-2009.
Querol, X., Pérez, N., Reche, C., Ealo, M., Ripoll, A., Tur, J., Pandolfi, M., Pey, J., Salvador, P., Moreno, T., Alastuey, A., 2019. African dust and air quality over Spain: Is it only dust that matters? Sci. Total Environ. 686, 737–752. https://doi.org/10.1016/J.SCITOTENV.2019.05.349.
Regayre, L.A., Johnson, J.S., Yoshioka, M., Pringle, K.J., Sexton, D.M.H., Booth, B.B.B., Lee, L.A., Bellouin, N., Carslaw, K.S., 2018. Aerosol and physical atmosphere model parameters are both important sources of uncertainty in aerosol ERF. Atmos. Chem. Phys. 18 (13), 9975–10006. https://doi.org/10.5194/acp-18-9975-2018.
Renard, J.-B., Dulac, F., Durand, P., Bourgeois, Q., Denjean, C., Vignelles, D., Couté, B., Jeannot, M., Verdier, N., Mallet, M., 2018. In situ measurements of desert dust particles above the western Mediterranean Sea with the balloon-borne Light Optical Aerosol Counter/sizer (LOAC) during the ChArMEx campaign of summer 2013. Atmos. Chem. Phys. 18 (5), 3677–3699. https://doi.org/10.5194/acp-18-3677-2018.
Reynolds, R.L., Goldstein, H.L., Moskowitz, B.M., Bryant, A.C., Skiles, S.M., Kokaly, R.F., Flagg, C.B., Yauk, K., Berquó, T., Breit, G., Ketterer, M., Fernandez, D., Miller, M.E., Painter, T.H., 2014. Composition of dust deposited to snow cover in the Wasatch Range (Utah, USA): Controls on radiative properties of snow cover and comparison to some dust-source sediments. Aeolian Res. 15, 73–90. https://doi.org/10.1016/j.aeolia.2013.08.001.
Rodá, F., Bellot, J., Avila, A., Escarré, A., Piñol, J., Terradas, J., 1993. Saharan dust and the atmospheric inputs of elements and alkalinity to mediterranean ecosystems. Water, Air, Soil Pollut. 66, 277–288. https://doi.org/10.1007/BF00479851.
Rodríguez, S., Querol, X., Alastuey, A., Kallos, G., Kakaliagou, O., 2001. Saharan dust contributions to PM10 and TSP levels in Southern and Eastern Spain. Atmos. Environ. 35 (14), 2433–2447. https://doi.org/10.1016/S1352-2310(00)00496-9.
Roettig, C.-B., Varga, G., Sauer, D., Kolb, T., Wolf, D., Makowski, V., Espejo, J.M.R., Zöller, L., Faust, D., 2018. Characteristics, nature, and formation of palaeosurfaces within dunes on Fuerteventura. Quat. Res. 1–20. https://doi.org/10.1017/qua.2018.52.
Rogora, M., Mosello, R., Marchetto, A., 2004. Long-term trends in the chemistry of atmospheric deposition in Northwestern Italy: the role of increasing Saharan dust deposition. Tellus B Chem. Phys. Meteorol. 56, 426–434. https://doi.org/10.3402/tellusb.v56i5.16456.
Rolph, G., Stein, A., Stunder, B., 2017. Real-time Environmental Applications and Display sYstem: READY. Environ. Model. Softw. 95, 210–228. https://doi.org/10.1016/j.envsoft.2017.06.025.
Sala, J.Q., Cantos, J.O., Chiva, E.M., 1996. Red dust rain within the Spanish Mediterranean area. Clim. Change 32 (2), 215–228. https://doi.org/10.1007/BF00143711.
Salvador, P., Alonso-Pérez, S., Pey, J., Artíñano, B., de Bustos, J.J., Alastuey, A., Querol, X., 2014. African dust outbreaks over the western Mediterranean Basin: 11-year characterization of atmospheric circulation patterns and dust source areas. Atmos. Chem. Phys. 14, 6759–6775. https://doi.org/10.5194/acp-14-6759-2014.
Schulz, M., Prospero, J.M., Baker, A.R., Dentener, F., Ickes, L., Liss, P.S., Mahowald, N.M., Nickovic, S., García-Pando, C.P., Rodríguez, S., Tegen, I., Duce, R.A., 2012. Atmospheric transport and deposition of mineral dust to the ocean: Implications for research needs. Environ. Sci. Technol. 46, 10390–10404. https://doi.org/10.1021/es300073u.
Smoydzin, L., Teller, A., Tost, H., Fnais, M., Lelieveld, J., 2012. Impact of mineral dust on cloud formation in a Saharan outflow region. Atmos. Chem. Phys. 12, 11383–11393. https://doi.org/10.5194/acp-12-11383-2012.
Sokolik, I.N., Toon, O.B., 1996. Direct radiative forcing by anthropogenic airborne mineral aerosols. Nature 381, 681–683. https://doi.org/10.1038/381681a0.
Stein, A.F., Draxler, R.R., Rolph, G.D., Stunder, B.J.B., Cohen, M.D., Ngan, F., 2015. Noaa's hysplit atmospheric transport and dispersion modeling system. Bull. Am. Meteorol. Soc. https://doi.org/10.1175/BAMS-D-14-00110.1.
Stuut, J.B., Smalley, I., O'Hara-Dhand, K., 2009. Aeolian dust in Europe: African sources and European deposits. Quat. Int. 198 (1–2), 234–245. https://doi.org/10.1016/j.quaint.2008.10.007.
Szoboszlai, Z., Kertész, Z., Szikszai, Z., Borbély-Kiss, I. and Koltay, E.: Ion beam microanalysis of individual aerosol particles originating from Saharan dust episodes observed in Debrecen, Hungary, Nucl. Instruments Methods Phys. Res. Sect. B Beam Interact. with Mater. Atoms, 267(12–13), 2241–2244, doi:10.1016/j.nimb.2009.03.019, 2009.
Tobías, A., Pérez, L., Díaz, J., Linares, C., Pey, J., Alastruey, A., Querol, X., 2011. Short-term effects of particulate matter on total mortality during Saharan dust outbreaks: A case-crossover analysis in Madrid (Spain). Sci. Total Environ. 412–413, 386–389. https://doi.org/10.1016/j.scitotenv.2011.10.027.
Tomadin, L., Lenaz, R., Landuzzi, V., Mazzucoletti, A., Vannucci, R., 1984. Wind-blown dust over the central Mediterranean. Oceanol. Acta 7, 13–23.
Twomey, S., 1974. Pollution and the planetary albedo. Atmos. Environ. 8, 1251–1256. https://doi.org/10.1016/0004-6981(74)90004-3.
van der Does, M., Knippertz, P., Zschenderlein, P., Giles Harrison, R., Stuut, J.-B.W., 2018. The mysterious long-range transport of giant mineral dust particles. Sci. Adv. 4 (12), eaau2768. https://doi.org/10.1126/sciadv.aau2768.
Varga, G., Roettig, C.-B., 2018. Identification of Saharan dust particles in Pleistocene dune sand- paleosol sequences of Fuerteventura (Canary Islands). Hungarian Geogr. Bull. 67 (2), 121–141. https://doi.org/10.15201/hungeobull.67.2.2.
Varga, G., 2012. Spatio-temporal distribution of dust storms - A global coverage using NASA TOMS aerosol measurements, Hungarian. Geogr. Bull. 61 (4).
Varga, G., Kovács, J., Újvári, G., 2013. Analysis of Saharan dust intrusions into the Carpathian Basin (Central Europe) over the period of 1979–2011. Glob. Planet. Change 100. https://doi.org/10.1016/j.gloplacha.2012.11.007.
Varga, G., Újvári, G., Kovács, J., 2014a. Spatiotemporal patterns of Saharan dust outbreaks in the Mediterranean Basin. Aeolian Res. 15. https://doi.org/10.1016/j.aeolia.2014.06.005.
Varga, G., Cserháti, C., Kovács, J., Szeberényi, J. and Bradák, B.: Unusual Saharan dust events in the Carpathian Basin (Central Europe) in 2013 and early 2014, Weather, 69(11), doi:10.1002/wea.2334, 2014b.
Varga, G., Cserháti, C., Kovács, J., Szalai, Z., 2016. Saharan dust deposition in the Carpathian Basin and its possible effects on interglacial soil formation. Aeolian Res. 22. https://doi.org/10.1016/j.aeolia.2016.05.004.
Varga, G., Kovács, J., Szalai, Z., Cserháti, C., Újvári, G., 2018. Granulometric characterization of paleosols in loess series by automated static image analysis. Sediment. Geol. 370, 1–14. https://doi.org/10.1016/j.sedgeo.2018.04.001.
Vieno, M., Heal, M.R., Twigg, M.M., MacKenzie, I.A., Braban, C.F., Lingard, J.J.N., Ritchie, S., Beck, R.C., Móring, A., Ots, R., Di Marco, C.F., Nemitz, E., Sutton, M.A., Reis, S., 2016. The UK particulate matter air pollution episode of March–April 2014: more than Saharan dust. Environ. Res. Lett. 11 (4), 044004. https://doi.org/10.1088/1748-9326/11/4/044004.
Wagenbach, D., Geis, K., 1989. The mineral dust record in a high alpine glacier (Colle Gnifett, Swiss Alps). In: Leinen, M., Sarnthein, M. (Eds.) Paleoclimatology and paleometeorology: modern and past patterns of global atmospheric transport. Kluwer, Dordrecht, pp. 543-564.
Washington, R., Todd, M., Middleton, N.J., Goudie, A.S., 2003. Dust-storm source areas determined by the total ozone monitoring spectrometer and surface observations. Ann. Assoc. Am. Geogr. 93 (2), 297–313. https://doi.org/10.1111/1467-8306.

9302003.
Weinzierl, B., Ansmann, A., Prospero, J.M., Althausen, D., Benker, N., Chouza, F., Dollner, M., Farrell, D., Fomba, W.K., Freudenthaler, V., Gasteiger, J., Groß, S., Haarig, M., Heinold, B., Kandler, K., Kristensen, T.B., Mayol-Bracero, O.L., Müller, T., Reitebuch, O., Sauer, D., Schäfler, A., Schepanski, K., Spanu, A., Tegen, I., Toledano, C., Walser, A., 2017. The Saharan aerosol long-range transport and aerosol-cloud-interaction experiment: Overview and selected highlights. Bull. Am. Meteorol. Soc. 98 (7), 1427–1451. https://doi.org/10.1175/BAMS-D-15-00142.1.
Yaalon, D.H., 1997. Soils in the Mediterranean region: what makes them different? Catena 28, 157–169. https://doi.org/10.1016/S0341-8162(96)00035-5.
Yaalon, D.H., Ganor, E., 1973. The influence of dust on soils during the quaternary. Soil Sci. 116, 146–155. https://doi.org/10.1097/00010694-197309000-00003.
Yu, H., Kaufman, Y.J., Chin, M., Feingold, G., Remer, L.A., Anderson, T.L., Balkanski, Y., Bellouin, N., Boucher, O., Christopher, S., DeCola, P., Kahn, R., Koch, D., Loeb, N., Reddy, M.S., Schulz, M., Takemura, T., Zhou, M., 2006. A review of measurement-based assessments of the aerosol direct radiative effect and forcing. Atmos. Chem. Phys. 6, 613–666. https://doi.org/10.5194/acp-6-613-2006.
Yu, H., Tan, Q., Chin, M., Remer, L.A., Kahn, R.A., Bian, H., Kim, D., Zhang, Z., Yuan, T., Omar, A.H., Winker, D.M., Levy, R.C., Kalashnikova, O., Crepeau, L., Capelle, V., Chédin, A., 2019. Estimates of African Dust Deposition Along the Trans-Atlantic Transit Using the Decadelong Record of Aerosol Measurements from CALIOP, MODIS, MISR, and IASI. J. Geophys. Res. Atmos. 124 (14), 7975–7996. https://doi.org/10.1029/2019JD030574.